HHS Public Access

Author manuscript

Adv Mater. Author manuscript; available in PMC 2018 September 01.

Published in final edited form as:

Adv Mater. 2017 September ; 29(33): . doi:10.1002/adma.201701255.

Nanostructured Mineral Coatings Stabilize Proteins for Therapeutic Delivery

Dr. Xiaohua Yu,
Department of Orthopedics and Rehabilitation, University of Wisconsin, Madison, WI 53705

Dr. Adam H. Biedrzycki,
Comparative Orthopedic Research Laboratory, School of Veterinary Medicine, University of Wisconsin-Madison, Madison, WI 53705

Mr. Andrew S Khalil,
Department of Biomedical Engineering, University of Wisconsin, Madison, WI 53706, USA

Mr. Dalton Hess,
Department of Biomedical Engineering, University of Wisconsin, Madison, WI 53706, USA

Mrs. Jennifer M. Umhoefer,
Department of Biology, University of Wisconsin, Madison, WI, 53705

Prof. Mark D. Markel, and
Comparative Orthopedic Research Laboratory, School of Veterinary Medicine, University of Wisconsin-Madison, Madison, WI 53705

Prof. William L. Murphy
Department of Orthopedics and Rehabilitation, University of Wisconsin, Madison, WI 53705

Department of Biomedical Engineering, University of Wisconsin, Madison, WI 53706, USA

Abstract

Proteins tend to lose their biological activity due to their fragile structural conformation during formulation, storage and delivery. Thus, the inability to stabilize proteins in controlled-release systems represents a major obstacle in drug delivery. Here we present a bone mineral inspired protein stabilization strategy, which uses nanostructured mineral coatings on medical devices. Proteins bound within the nanostructured coatings demonstrated enhanced stability against extreme external stressors, including organic solvents, proteases, and ethylene oxide gas sterilization. The protein stabilization effect was attributed to the maintenance of protein conformational structure, which was closely related to the nanoscale feature sizes of the mineral coatings. Basic fibroblast growth factor (bFGF) released from a nanostructured mineral coating maintained its biological activity for weeks during release, while it maintained activity for less than seven days during release from commonly used polymeric microspheres. Delivery of the growth factors bFGF and vascular endothelial growth factor (VEGF) using a mineral coated

Correspondence to: William L. Murphy.

Competing financial interests
The authors declare no competing financial interests.

surgical suture significantly improved functional Achilles tendon healing in a rabbit model, resulting in increased vascularization, more mature collagen fiber organization, and a 2-fold improvement in mechanical properties. Our findings demonstrate that biomimetic interactions between proteins and nanostructured minerals provide a new, broadly applicable mechanism to stabilize proteins in the context of drug delivery and regenerative medicine.

Keywords

Nanostructure; Protein stability; Mineral coating; Therapeutics; Protein delivery

The rise of therapeutic protein applications in the pharmaceutical industry has attracted much attention due to their specificity and potency relative to small molecule drugs[1]. However, this also poses a major challenge in formulation and delivery of proteins, due to their complex intramolecular folding and susceptibility to denaturation and degradation[2,3]. Over the past three decades, investigators have attempted to address these problems by encapsulating proteins into bioresorbable polymer matrices such as scaffolds, microspheres, and nanoparticles [4–6]. While these strategies have achieved sustained release, the intrinsic instability of protein therapeutics against various external stresses during formulation and delivery remains a significant challenge. Proteins incorporated into a polymeric carrier are exposed to a series of stresses, such as hydrophobic interfaces, vigorous agitation, and detergents during formulation. They are also challenged by elevated temperature, polymer degradation byproducts and increased levels of moisture during delivery[7]. Previous studies have shown that proteins encapsulated in polymer carriers were significantly agglomerated and lost their therapeutic functionality[8,9]. For instance, Zhu et al. reported that the instability of protein trapped in polymer matrix was due in part to the acidic microclimate inside the polymer matrix[8]. Cicerone *et al.* revealed that accelerated β-relaxation of protein chains in a high moisture microenvironment could expedite protein degradation[10]. Few strategies have been developed to stabilize the cargo proteins during formulation, storage and release, and thereby overcome these limitations in current protein delivery systems.

It is known that natural bone tissue can preserve biological macromolecules embedded within the bone matrix for thousands of years after the death of an individual[11]. Archaeologists have successfully extracted intact proteins such as growth factors and other non-collagenous proteins from human bones and teeth from the early Middle Ages[12,13]. This remarkable protein preservation effect can be partially attributed to the unique physiochemical properties of the bone tissue extracellular matrix. In particular, non-collagenous proteins in bone are tightly bound to nanostructured hydroxyapatite mineral crystals, which comprise the main inorganic component of bone[14,15]. The bone mineral effectively protects the proteins against attacks from various physical and chemical stresses postmortem[16]. We reasoned that this natural phenomenon of long term protein preservation in mineralized tissues may provide a mechanism to stabilize protein therapeutics during sustained release, and circumvent the limitations associated with current protein delivery strategies.

We hypothesized that electrostatic interactions between side chains on the protein and the ionic surface of a mineral coating could confine the mobility of protein chains and stabilize the protein against various external stresses. To demonstrate this concept, we generated a series of biomimetic mineral surfaces on medical device substrates, including microparticles and surgical sutures. We showed that protein stability against external stressors was substantially increased upon binding of protein to the nanostructured mineral. Using bFGF as an example, we further demonstrated that its biological activity can be stabilized for up to five weeks during release from a mineral-coated device, while it can only be maintained for seven days during release from polymer microspheres. Importantly, the protein stabilizing mineral coatings could be readily applied to common medical devices, which we demonstrated here by generating growth factor-releasing sutures that could be sterilized while maintaining growth factor activity and used to stimulate enhanced functional healing in a rabbit Achilles tendon resection model.

Results and discussion

Nanostructured mineral coatings were formed on microparticles via incubation in modified simulated body fluids (mSBFs), as demonstrated in previous studies [17–19] (Fig. 1-A). The resultant mineral coatings exhibited a plate-like nanostructure which mimics some structural characteristics of natural bone mineral (Fig. 1-B). A cross sectional view of the mineral-coated microparticles (MCMs) revealed nanostructured porosity throughout the ~2 μm coating thickness, which endowed the MCMs with a high surface area favorable for protein binding (Fig. 1-C). The MCM were a versatile platform for various protein binding, showing binding of horse radish peroxidase (HRP), bovine serum albumin (BSA), and basic fibroblast growth factor (bFGF) (Fig. S-1). We hypothesized that protein binding on mineral coatings was via electrostatic interactions between protein side chains and the charged surface on mineral coating, which was supported by the correlation between bFGF release and ionic strength in release buffer (Fig. S-2). The generic protein binding mechanism suggests that this approach may be adaptable to a broad range of therapeutic proteins.

Nanostructured mineral coatings significantly improved stability of HRP against denaturation in the presence of an organic solvent. Proteins are often exposed to an aqueous-organic interface during various formulation processes such as emulsion or coacervation[20]. To mimic this scenario in an extreme fashion, we vortexed a solution containing HRP in PBS and ethyl acetate (EA), an organic solvent generally used in emulsion processing. Free HRP in PBS retained only 68.0 ±8.9% of its initial enzymatic activity after 2 h of exposure, and the remaining HRP activity continued to decrease to 37.2±11.0% after 4h. Only 11.1±0.3% of HRP activity was preserved by the end of a 24 h EA treatment. In contrast, HRP bound on MCM retained 93.5±11.1% of its activity after 2 h EA treatment and the remaining activity at 4h was maintained at 71.6±21.5%. The HRP activity on MCM at 24 h was 30.8±9.3%, approximately 2.5-fold higher than HRP activity in PBS (Fig. 1-D). We next exposed HRP bound on MCM to a broad range of organic solvents with different polarity indices for 4 h (Fig. 1-E). Regardless of the solvent polarity, HRP bound on MCM exhibited significantly higher activity (up to 6-fold increased activity) compared to HRP in PBS, implying the stabilization of protein in the MCM is widely adaptable to various solvents known to induce protein denaturation.

Nanostructured mineral coatings also significantly improved biological activity of proteins incorporated within, and released from, biomaterials. To explore the ability of mineral coatings to stabilize proteins during incorporation and release, we first directly compared enzymatic activity of HRP encapsulated and released from commonly used poly (lactide-co-glycolide) (PLG) microspheres to HRP bound and released from mineral coated PLG microspheres (Fig. S-3). The activity of HRP encapsulated and released from PLG microspheres was only 18.5 ± 3.5% of fresh HRP in PBS, while HRP bound and released from mineral coated PLG microspheres showed no significant loss of enzymatic activity compared to HRP in PBS (Fig. 1-F). This result indicated that mineral could serve as a carrier to preserve protein activity during formulation of a sustained release system.

To gain further insights into the protein stabilizing effects of mineral coatings, we next investigated the structural change of proteins in the presence of external stressors in PBS buffer and on mineral coatings. Bovine serum albumin (BSA) rapidly precipitated upon exposure to organic solvents including with various polarities, as expected. This experiment observed BSA precipitation was significantly decreased when BSA was bound to MCM (Fig. 2-A). Since protein precipitation typically results from aggregation of denatured proteins [21], we reasoned that BSA bound to mineral coatings would also be less likely to denature in presence of organic solvent. Indeed, acetone caused severe disruption of the secondary structure of BSA in PBS, as shown in the circular dichroism (CD) spectrum (Fig. S-4). Importantly, BSA showed more severe disruption of α-helix content (peaks at 208 and 222 nm) in PBS when compared to BSA bound to MCM, indicating that BSA bound on MCM was more resistant to structural disruption (Fig. 2-B&C). In view of these observations, we speculated that nanostructured mineral coatings may serve as a protein immobilization matrix, which provides the protein side chains with numerous anchor points. While organic solvent molecules can freely attack any region of the soluble protein in PBS, the interactions between the mineral coating and the protein side chains may increase the rigidity of the protein conformation and its resistance to mis-folding[22]. Protein immobilization on MCMs might also prevent mis-folded protein from aggregating, as protein molecules on MCM lose their mobility and have limited access to each other (Fig. 2-D). These data collectively imply that mineral coatings are capable of preserving protein secondary structure thus preventing protein molecules from denaturing and aggregating.

We next modified the characteristics of the mineral coatings to determine whether the mineral coating nanostructure could influence protein stabilization against extreme stressors. As the carbonate concentration in mSBF was increased from 4.2 mM to 150 mM, the size of the nanoscale features of the mineral coatings gradually decreased from ~1 μm to ~100 nm (Fig. 3-A)[23,24]. Upon challenge with EA solution, HRP enzymatic activities on each mineral coating were found to be significantly higher than HRP enzymatic activities in PBS. Interestingly, there was also a direct dependence of the remaining HRP activity after EA challenge on the nanostructure of the coatings. In particular, an increasing trend of HRP stabilization was evident with a decrease in the nanostructure feature size of the mineral coatings from ~1 μm to ~100 nm (Fig. 3-B). Based on this result, we hypothesize that as the size of the nano-porous structures dropped from 1μm down to 100 nm, the effective protein confinement might increase, leading to enhanced stabilization of protein against denaturing organic solvents (Fig. 3-C). This possible hypothesis supports classical protein

conformational stabilization theory, which states that proteins supported by a matrix through strong chemical bonds are less likely to be unfolded, and therefore less likely to be denatured[25].

Next, we extended this protein stabilization strategy to growth factors, which are potent regulators of biological processes including cell proliferation and tissue regeneration[26–28]. We specifically evaluated vasic fibroblast growth factor (bFGF) activity due to its extreme instability during storage and delivery[20,29]. Human dermal fibroblast cells (hDF) proliferation was initially used as an *in vitro* assay to evaluate bFGF activity (Fig. S-5), as bFGF could stimulate growth of hDF populations by 2.2-fold and 3.7-fold when added at 1 and 10 ng/ml, respectively. After challenging bFGF in PBS with EA, bFGF substantially lost biological activity and only promoted hDF growth by 1.4-fold and 1.3-fold at 1 and 10 ng/ml, respectively (Fig. 4-A&B). In contrast, bFGF bound on MCM and challenged with EA treatment could still stimulate hDF proliferation, as the bFGF on MCM after EA exposure stimulated hDF growth by 2.2-fold at 1 ng/ml (Fig. 4-C&D, and Fig. S-6). Similar bFGF stabilization effects on MCM were also observed when other commonly used organic solvents were used as stressors (Fig. 4-E). The only exception was Hexanes (Hex), which is a non-polar organic solvent and showed no destructive impact on bFGF activity. The loss of bFGF biological activity on MCM was proportional to the solvent polarity, with more polar solvents causing greater decreases in bFGF bioactivity (Fig. 4-E). This suggests that the hydrophilic surface of MCM may provide more accessibility to more highly polar solvents[30]. Importantly, bFGF stabilization also demonstrated a nanostructure-dependence similar to that demonstrated for HRP (Fig. 1-E), as mineral coatings with smaller nanostructural features enabled greater bFGF stabilization (Fig. 4-F). Finally, we found that MCM also helped to preserve bFGF activity through multiple cycles of freeze drying (Fig. S-7), suggesting nanostructured minerals could serve as stabilizers during protein formulation and storage (Fig. 4-G).

Protease activity is another type of challenge faced by therapeutic protein during delivery. We found that bFGF bound on MCM showed very little activity loss after 0.05% trypsin treatment for 2 hours while soluble bFGF in PBS with 0.05% trypsin lost over 50% of its original activity (Fig. 4-H). To further explore the broader applicability of the mineral coatings, we next formed mineral coatings on one of the most commonly used clinical biomaterials, absorbable collagen sponge (ACS). Mineral coated ACS (MCACS) (Fig. S-8) bound bFGF and showed higher bFGF activity after ethyl acetate treatment compared to non-coated ACS (Fig. 4-I), suggesting that the protein stabilization effect of mineral can be broadly applied to commonly used medical devices to improve their efficacy.

bFGF released from nanostructured mineral coatings maintained its biological activity during sustained release, in contrast to the relatively poor biological activity of bFGF released from commonly used polymer microspheres. Specifically, we directly compared the long term biological activity of bFGF encapsulated into PLG microspheres *via* standard water-in-oil-in-water double emulsion (denoted as “ PLG ”), or bound onto nanostructured mineral coatings formed upon PLG microspheres (denoted as “ PLG/MCM ”) (Fig. 5-A). In order to conduct a direct comparison between these two bFGF delivery approaches, we loaded the same amount of bFGF (13 ng bFGF/mg microspheres) onto the same mass of the

two types of microspheres, based on their measured protein loading efficiencies (Fig. S-9). Sustained release of radiolabeled bFGF from both types of microspheres was detected for more than 35 days, and the two different types of microspheres showed similar release profiles (Fig. 5-B). PLG microspheres showed a somewhat higher release rate of over 90% of encapsulated bFGF by day 35 versus 65% of bound bFGF released from PLG/MCM by day 35 (Fig. 5-B). bFGF from both types of microspheres could stimulate hDF growth, and no statistical difference was noticed at day 3 in terms of hDF population growth in response to released bFGF. After that, the Transwells® containing the bFGF loaded microspheres were transferred once every 3–5 days into new wells seeded with hDFs to track the biological activity of the released bFGF over a sustained timeframe. During days 4–6, bFGF released from PLG only stimulated cell growth by 157.9 ± 9.2%, while bFGF released from PLG/MCM increased the cell growth by 274.4 ± 10.7%. Importantly, bFGF released from PLG microspheres showed no effect on hDF population growth after day 6, indicating that any additional bFGF released beyond day 6 was not biologically active. In contrast, bFGF released from PLG/MCM continued to promote hDF population growth for the duration of the 35 day release assay (Fig. 5-C&E).

Notably, the bioactivity of bFGF released from PLG/MCM could be maintained for up to 10 days even after EA treatment at day 0, which is still significantly longer than the bFGF activity during release from PLG microspheres (Fig. 5-D). Our results for PLG microspheres are consistent with previous studies, which have shown that proteins incorporated into these conventional polymeric carriers tend to aggregate and lose their activity during sustained incubation in physiological conditions[8,9]. However, the results for PLG/MCM release suggest a broadly applicable new mechanism for sustained release of proteins with extended maintenance of biological activity.

The clinical impact of growth factors in regenerative medicine applications has been severely limited due to their extreme instability during storage and use. We next investigated whether the ability of nanostructured mineral coatings to stabilize growth factors could augment biological activity of growth factors during rabbit Achilles tendon healing (Fig. 6-A). Standard surgical sutures were coated with a mineral layer with nanostructural features similar to those formed on MCMs (Fig. 6-B), resulting in formation of mineral coated sutures. bFGF was released in a sustained manner from mineral coated sutures (Fig. 6-C), and the same approach was used to form multi-layered mineral coatings for dual release of bFGF and vascular endothelial growth factor (VEGF) (Fig. 6-D), as described previously[31]. Coated sutures with incorporated bFGF or bFGF/VEGF were then sterilized with ethylene oxide gas, and used to repair a rabbit Achilles tendon defect. Tendon defects repaired with non-coated sutures showed hyper cellularity, round cells within the repair site, and random orientation of the newly formed collagen bundles, consistent with reactive scar tissue formation. Defects treated with bFGF-releasing or bFGF/VEGF-releasing sutures showed significantly increased blood vessel density, more organized collagen structure, and more mature tenocyte appearance (Fig. 6-E). Significantly more blood vessels were located close to the suture than further away from it, indicating the local release of growth factors stimulated vascularization in the defects (Fig. 6-F). Importantly, the ultimate tensile strength of the healed tendon in the bFGF/VEGF-releasing suture group (318.7±20.3N) more than doubled that of the control group (152.0±17.6 N) at 4 weeks (Fig. 6-G), indicating that

delivery of multiple growth factors using coated sutures can stimulate tendon healing without changing any other characteristics of the surgical procedure. These results show that coated sutures can release biologically active proteins and stimulate functional tendon healing even after ethylene oxide gas sterilization of the protein-loaded sutures.

Despite major advances in development of polymeric carriers as controlled release systems, few strategies have been successful in improving the biological activity of therapeutic proteins in the presence of extreme stressors or over the course of sustained release. In stark contrast, proteins embedded within the mineralized extracellular matrix of natural bone tissue can be preserved for centuries [12,13]. Here we reasoned that the mechanisms that enable protein stabilization in nature's mineralized tissues may provide a mechanism for therapeutic protein stabilization as well. Taken together, our studies demonstrated that nanostructured mineral coatings stabilize proteins against denaturation and aggregation in extreme conditions, and that smaller nanostructural features provide improved protein stabilization. This protein stabilization effect was applicable to multiple distinct proteins, and was used to produce long-term biological activity during sustained growth factor delivery *in vitro* and *in vivo*. The protein-mineral binding mechanism is generic to virtually any kind of protein[32,33], which suggests the approach may be applicable in multiple regenerative medicine applications. It is noteworthy that our results may be broadly consistent with other recent studies, in which protein confinement in nanocapsules[7], protein-mediated nucleation of inorganic crystals[34], or protein coating with heparin-mimetic macromolecules[35] have significantly improved protein stability. The mechanisms in these prior studies involved biochemical and/or biophysical maintenance of proper protein folding, which is similar to the mechanisms we have proposed in our current study.

Methods

Microspheres fabrication and mineral coating formation

PLG microspheres were fabricated using a water-in-oil-in-water (W/O/W) double-emulsion technique (see SI Materials and Methods). The plain PLG microspheres were prepared without addition of protein likewise. PLG microspheres were coated with a layer of mineral coating by incubating in mSBF with 100 mM NaHCO3 for 7 days similar to previous study[31]. mSBF was prepared bydissolving NaCl, KCl, $MgSO_4$, $MgCl_2$, $NaHCO_3$, $CaCl_2$, KH_2PO_4, and Tris.HCl in DI water, and pH was adjusted by adding HCl and NaOH solution to 7.40. The resulting mineral coated PLG microspheres were filtered through a 35 μm cell strainer to exclude the large aggregates. The collected mineral coated PLG microspheres was lyophilized and stored at −20 °C freezer.

In another experiment, hydroxyapatite microparticles with diameter between 3~5 μm (Plasma Biotal LTD, UK) were incubated in mSBF (pH 6.80) to form a layer of mineral coating covering the microparticles. Each 100 mg hydroxyapatite microparticles were incubated in 50 mL mSBF at 37 °C for 7 days with daily solution refreshment. All MCM except nanostructure screen were grown in mSBF with 100 mM $NaHCO_3$. For MCM nanostructure screening, the concentration of $NaHCO_3$ was systematically changed from 4.2 to 150 mM (Table S-1). The resultant MCM were washed in de-ionized water and lyophilized.

Protein binding on MCMs

For BSA, each of 5.0 mg MCMs was incubated in 1.0 mL 100 μg/mL of BSA in PBS at 37 °C for 4 h with rotation. After binding, the remaining concentration of BSA in the solution was measured by microBCA protein assay (Thermo Fisher, Rockford, IL).

For HRP, each of 5.0 mg MCMs was incubated in 1.0 mL 10 μg/mL of HRP in PBS at 37 °C for 4 h with rotation. After binding, the remaining concentration of HRP in the solution was measured by microBCA protein assay (Thermo Fisher, Rockford, IL). For bFGF, radiolabeled bFGF (125I-labeled bFGF) was used to determine the binding efficiency. Briefly, each of 5.0 mg MCMs was incubated in 1.0 mL 10 ng/mL or 100 ng/mL bFGF (with 0.1% 125I bFGF) in PBS at 37 °C for 4 h with rotation. The MCMs were then centrifuged at 11,000 g for 2 min and washed with 1.0 mL PBS once. The radioactivity in the supernatant and washing PBS was measured by a Packard Cobra II Gamma Counter (Perkin Elmer, Waltham, MA) to determine the remaining bFGF concentration after binding. All protein binding efficiencies were calculated from the protein concentration change before and after binding.

Stability study of proteins bound on MCM against external stresses

Various proteins were used to bind to mineral coating (see SI Materials and Methods), and exposed to different external stressors.800 μL organic solvent was added into 5.0 mg protein bound MCM or 200 μL protein solution in PBS in a 1.5 mL centrifuge tube and the mixture was kept vortexing for different time periods. Control groups without addition of solvent were prepared accordingly. The solvent was then removed by vacuum drying after treatment and all the samples were reconstituted with PBS. The secondary structure of BSA after organic solvents treatment was measured by a circular dichroism spectrometer (Model 420, Aviv) (Lakewood, NJ) at 20 °C.

In another experiment, 1.0 mL 0.05% trypsin was added into 5.0 mg bFGF bound MCM or 10 μL 100 μg/mL bFGF in PBS in a 1.5 mL centrifuge tube and the mixture was kept rotating at 37°C for 1 h. Control groups without trypsin treatment were prepared to calculate the loss of bFGF activity. After the treatment, trypsin was removed from MCM-containing groups and MCM was resuspended in medium. bFGF in PBS was diluted to 100 ng/mL using medium and added to hDF culture at a final concentration of 1.0 ng/mL. Reconstituted proteins samples were then subjected for their activity measurement using specific assay for each type of protein (see SI Materials and Methods).

BSA circular dichroism (CD) spectra measurement

The secondary structure of BSA after organic solvents treatment was measured by a circular dichroism spectrometer (Model 420, Aviv) (Lakewood, NJ) at 20 °C. BSA recovered from various treatments was quantified and diluted to 100 μg/mL in PBS. CD spectra were recorded with a 1 mm path length quartz curvette. Data were acquired at bandwidth of 1.0 nm, response of 3 s and each measurement was repeated at least three times and the average value was plotted.

bFGF bioactivity evaluation

Human dermal fibroblast (hDF) was maintained in Dulbecco's Modified Eagle's Medium (DMEM) supplemented with 2% fetal calf serum, 100 unit/ml penicillin and 100 μg/ml streptomycin aMethot 37 °C with 5% CO2. The medium was changed every other day and hDF were used up to passage 11.

To facilitate hDF adhesion in serum free medium, 24-well plate was coated with 0.1% gelatin for 2 h before cell seeding. hDF were harvested from T75 flasks after trypsinization and resuspended in UltraCulture serum-free medium supplemented with 2 mM L-glutamine, 100 unit/ml penicillin and 100 μg/ml streptomycin. The cells were seeded into gelatin coated 24-well plates at 10,000/well and incubated for overnight to allow cell attachment. For untreated/treated bFGF in PBS, final bFGF concentrations of 1.0 and 10.0 ng/mL were used to induce hDF proliferation. For untreated/treated bFGF bound on MCMs, 3.0 mg MCMs containing different amount of bFGF was suspended in 200 μL serum-free medium and added into a transwell placed on top of hDF (Fig S-3). After 72 h of culture, CellTiter-Blue Viability Assay (Promega, WI) was conducted to evaluate the proliferation of hDF. The group received only blank medium was used as the control group and all the experimental groups were normalized to the control group. Each group contains four replicates.

Evaluation of bFGF activity released from different particles

bFGF encapsulated PLG microspheres (~13 ng/mg) were fabricated using a W/O/W double emulsion[19]. Plain PLG microspheres were coated with MCMSs using the same procedure as previously described. bFGF was bound to MCMs at ~13 ng/mg calculated based on bFGF binding efficiency. 3.0 mg of each type of bFGF loaded microspheres was re-suspended in 200 μL UltraCulture medium and added into a transwell insert in a 24 well seeded with 10,000 hDF cells/well. At each time point, the Transwell insert was transferred into a new well seeded with the same number of hDF 12 h in advance. CellTiter Blue assay was performed to evaluate the growth of hDF in each group. hDF proliferation was normalized to the blank control which only received UltraCulture medium. Live/dead staining was conducted at each time point following CellTiter Blue assay.

Rabbit Achilles tendon healing model

The animal study was approved by the UW-Madison Animal Care and Use Committee (Protocol V01554). 4 month-old New Zealand while rabbits with average weight of 2–3 kg were used for this study (n=6). After anesthesia with isoflurane, a 15 mm skin incision was made centered 15 mm proximal to the calcaneus on the lateral aspect of the tibia, the lateral tendon was sharply transected 15 mm proximal to the calcaneus with a #15 scalpel blade. The transection was immediately repaired with a single locking loop of 4-0 braided nylon (Surgilon, Covidien, Mansfield, MA) coated with bone-like mineral containing different growth factor combinations. Once the body of the tendon was repaired, a circumferential repair of the paratenon was applied in a Silfaverskiold epitendinous reapir using using 4-0 braided polyglactin 910 (Vicryl, Ethicon, Cincinnati, OH) (also coated with same coating containing growth factors identical to the central core suture). The subcutaneous fascia was sutured using 6-0 polyglactin 910 (Vicryl, Ethicon, Cincinnati, OH) in a simple continuous pattern and the skin was sutured using 3-0 polypropylene (Prolene, Ethicon, Cincinnati, OH)

in a cruciate pattern. Biomechanical testing and histological analysis were performed after harvesting samples from the animals (see detailed protocols in SI Materials and Methods)

Supplementary Material

Refer to Web version on PubMed Central for supplementary material.

Acknowledgments

The authors acknowledge funding from the National Institutes of Health (Grant:R01AR059916), the National Institute of General Medical Sciences' Biotechnology Training Program (Grant: 5 T32-GM08349), and the National Science Foundation (Grant: DMR 1105591).

References

1. Mitragotri S, Burke PA, Langer R. Overcoming the challenges in administering biopharmaceuticals: formulation and delivery strategies. Nat Rev Drug Discov. 2014; 13:655–72. [PubMed: 25103255]
2. Fu K, Klibanov aM, Langer R. Protein stability in controlled-release systems. Nat Biotechnol. 2000; 18:24–5. [PubMed: 10625383]
3. Frokjaer S, Otzen DE. Protein drug stability: a formulation challenge. Nat Rev Drug Discov. 2005; 4:298–306. [PubMed: 15803194]
4. Chen RR, Mooney DJ. Polymeric growth factor delivery strategies for tissue engineering. Pharm Res. 2003; 20:1103–1112. [PubMed: 12948005]
5. Jeong B, Bae YH, Lee DS, Kim SW. Biodegradable block copolymers as injectable drug-delivery systems. Nature. 1997; 388:860–2. [PubMed: 9278046]
6. Richardson TP, Peters MC, Ennett AB, Mooney DJ. Polymeric system for dual growth factor delivery. Nat Biotechnol. 2001; 19:1029–1034. [PubMed: 11689847]
7. Giri J, Li WJ, Tuan RS, Cicerone MT. Stabilization of proteins by nanoencapsulation in sugar-glass for tissue engineering and drug delivery applications. Adv Mater. 2011; 23:4861–7. [PubMed: 21953536]
8. Zhu G, Mallery SR, Schwendeman SP. Stabilization of proteins encapsulated in injectable poly (lactide- co-glycolide). Nat Biotechnol. 2000; 18:52–7. [PubMed: 10625391]
9. Fu K, Griebenow K, Hsieh L, Klibanov AM, Langer R. FTIR characterization of the secondary structure of proteins encapsulated within PLGA microspheres. J Control Release. 1999; 58:357–66. [PubMed: 10099160]
10. Cicerone MT, Soles CL. Fast dynamics and stabilization of proteins: Binary glasses of trehalose and glycerol. Biophys J. 2004; 86:3836–3845. [PubMed: 15189880]
11. Asara JM, Schweitzer MH, Freimark LM, Phillips M, Cantley LC. Protein sequences from mastodon and Tyrannosaurus rex revealed by mass spectrometry. Science. 2007; 316:280–5. [PubMed: 17431180]
12. Schmidt-Schultz TH, Schultz M. Intact growth factors are conserved in the extracellular matrix of ancient human bone and teeth: a storehouse for the study of human evolution in health and disease. Biol Chem. 2005; 386:767–76. [PubMed: 16201872]
13. Schmidt-Schultz TH, Schultz M. Bone protects proteins over thousands of years: extraction, analysis, and interpretation of extracellular matrix proteins in archeological skeletal remains. Am J Phys Anthropol. 2004; 123:30–9. [PubMed: 14669234]
14. Palmer LC, Newcomb CJ, Kaltz SR, Spoerke ED, Stupp SI. Biomimetic systems for hydroxyapatite mineralization inspired by bone and enamel. Chem Rev. 2008; 108:4754–4783. [PubMed: 19006400]
15. Hartgerink JD, Beniash E, Stupp SI. Self-assembly and mineralization of peptide-amphiphile nanofibers. Science (80-). 2001; 294:1684–1688.
16. Collins M, Gernaey A, Nielsen-Marsh C, Vermeer C, Westbroek P. Slow rates of degradation of osteocalcin: Green light for fossil bone protein? Geology. 2000; 28:1139–1142.

17. Lee JS, Lu Y, Baer GS, Markel MD, Murphy WL. Controllable protein delivery from coated surgical sutures. J Mater Chem. 2010; 20:8894.
18. Suárez-González D, et al. Controlled nucleation of hydroxyapatite on alginate scaffolds for stem cell-based bone tissue engineering. J Biomed Mater Res Part A. 2010; 95:222–234.
19. Jongpaiboonkit L, Franklin-Ford T, Murphy WL. Mineral-Coated Polymer Microspheres for Controlled Protein Binding and Release. Adv Mater. 2009; 21:1960–1963.
20. Edelman ER, Mathiowitz E, Langer R, Klagsbrun M. Controlled and modulated release of basic fibroblast growth factor. Biomaterials. 1991; 12:619–26. [PubMed: 1742404]
21. Yoshikawa H, Hirano A, Arakawa T, Shiraki K. Mechanistic insights into protein precipitation by alcohol. Int J Biol Macromol. 2012; 50:865–871. [PubMed: 22115717]
22. Cao L. Immobilised enzymes: science or art? Curr Opin Chem Biol. 2005; 9:217–26. [PubMed: 15811808]
23. Choi S, Yu X, Jongpaiboonkit L, Hollister SJ, Murphy WL. Inorganic coatings for optimized non-viral transfection of stem cells. Sci Rep. 2013; 3:1567. [PubMed: 23535735]
24. Lee JS, Lu Y, Baer GS, Markel MD, Murphy WL. Controllable protein delivery from coated surgical sutures. J Mater Chem. 2010; 20:8894–8903.
25. Klibanov, aM. Enzyme stabilization by immobilization. Anal Biochem. 1979; 93:1–25. [PubMed: 35035]
26. Tayalia P, Mooney DJ. Controlled Growth Factor Delivery for Tissue Engineering. Adv Mater. 2009; 21:3269–3285. [PubMed: 20882497]
27. Xu RH, et al. Basic FGF and suppression of BMP signaling sustain undifferentiated proliferation of human ES cells. Nat Methods. 2005; 2:185–90. [PubMed: 15782187]
28. Yu X, Suárez-González D, Khalil AS, Murphy WL. How does the pathophysiological context influence delivery of bone growth factors? Adv Drug Deliv Rev. 2014; doi: 10.1016/j.addr.2014.10.010
29. Whalen GF, Shing Y, Folkman J. The fate of intravenously administered bFGF and the effect of heparin. Growth Factors. 1989; 1:157–64. [PubMed: 2624780]
30. Aronov D, Rosen R, Ron EZ, Rosenman G. Tunable hydroxyapatite wettability: Effect on adhesion of biological molecules. Process Biochem. 2006; 41:2367–2372.
31. Yu X, Khalil A, Dang PN, Alsberg E, Murphy WL. Multilayered InorganicMicroparticles for Tunable Dual Growth Factor Delivery. Adv Funct Mater. 2014; 24:3082–3093. [PubMed: 25342948]
32. Lee JS, Suarez-Gonzalez D, Murphy WL. Mineral Coatings for Temporally Controlled Delivery of Multiple Proteins. Adv Mater. 2011; 23:4279–4284. [PubMed: 22039597]
33. Suárez-González D, et al. Controllable mineral coatings on PCL scaffolds as carriers for growth factor release. Biomaterials. 2012; 33:713–721. [PubMed: 22014948]
34. Ge J, Lei J, Zare RN. Protein-inorganic hybrid nanoflowers. Nat Nanotechnol. 2012; 7:428–32. [PubMed: 22659609]
35. Nguyen TH, et al. A heparin-mimicking polymer conjugate stabilizes basic fibroblast growth factor. Nat Chem. 2013; 5:221–7. [PubMed: 23422564]

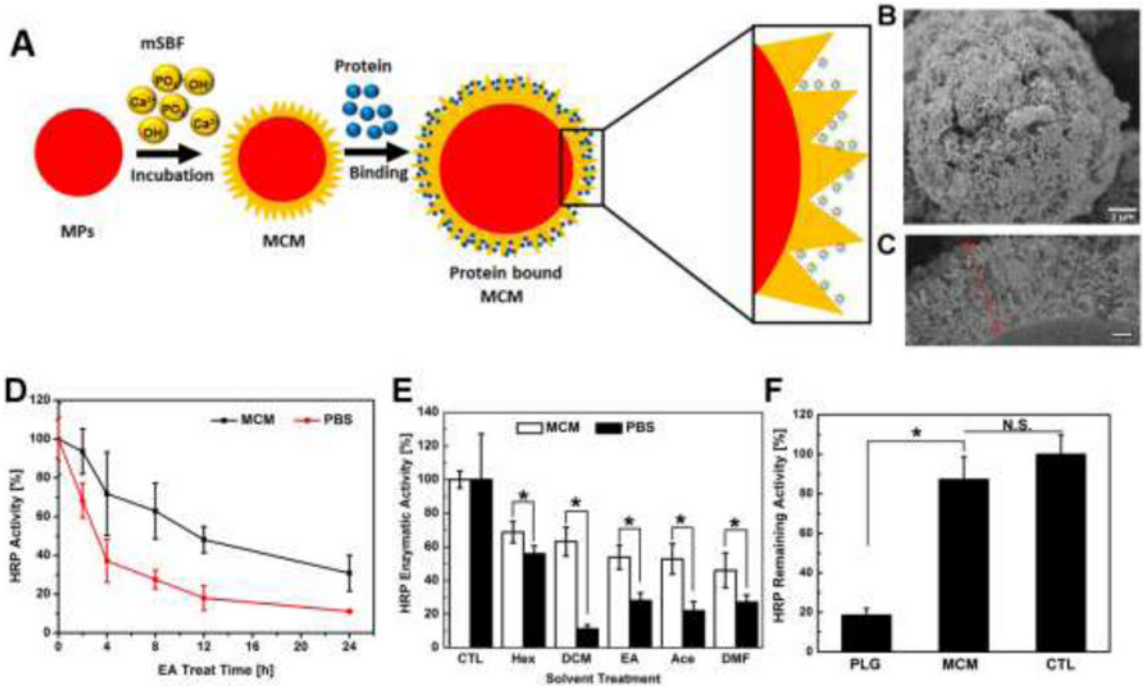

Figure 1. Protein stabilization via mineral-coated microparticles (MCM) using HRP as a model enzyme

A) Schematic illustration of protein binding on the MCM surface. Protein can be bound within the nanostructure of the mineral coating. B) Electron micrograph of the MCM uniformly covered with a layer of nanostructured mineral coating. C) SEM image of cross section view of the mineral coating: a nanoporous coating with thickness ~2 μm. D) HRP activity retention during organic solvent treatment. Both HRP in PBS and on MCM were treated with ethyl acetate (EA) for 24 h. The HRP activities of PBS and MCM at 0 h were set as 100%. E) Remaining HRP activity after various organic solvent treatments for 4 h. F) Comparison of released HRP activity between PLG microspheres and MCM: HRP released into PBS from both types of vehicles was quantified and their activity was tested via a TMB enzymatic assay.

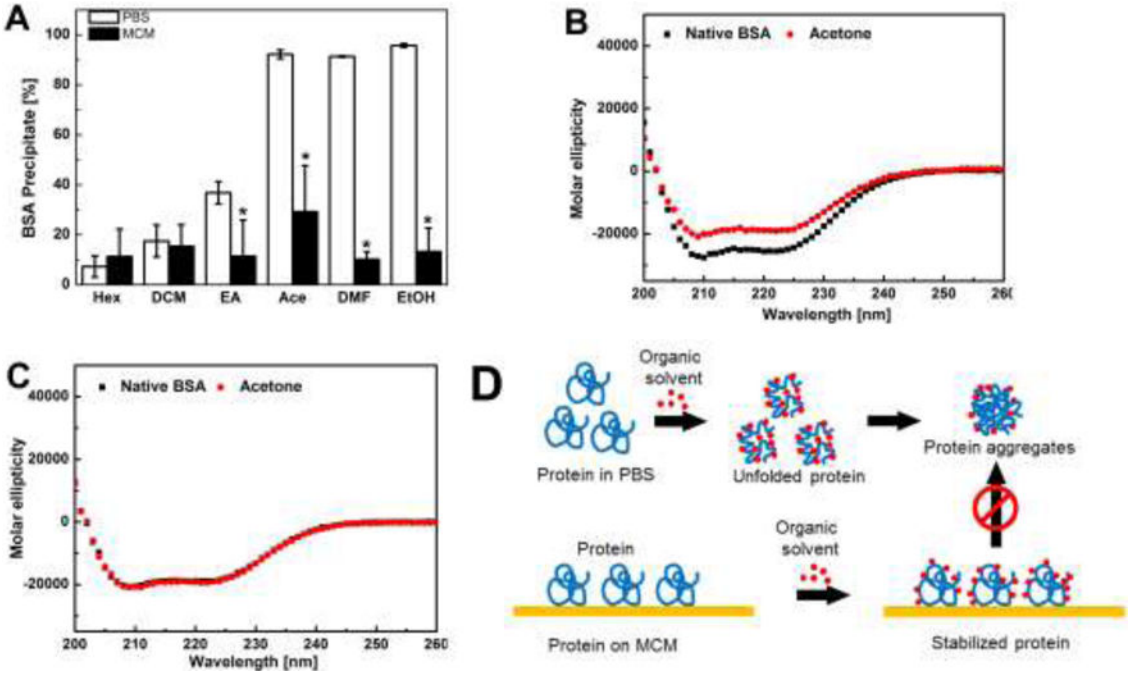

Figure 2. Structural analysis of protein denaturation via a model protein BSA

A) BSA precipitation after various organic solvents treatment: for protein in PBS, soluble protein was recovered from the buffer via centrifugation; for MCMs, soluble protein on MCMs was recovered by elution using phosphate buffer. data are presented as mean ± SD (n=6) *$p<0.05$; B) CD spectra of BSA in PBS before and after acetone treatment. C) CD spectra of BSA recovered from MCMs before and after acetone treatment. D) Proposed protein stabilization mechanism: interactions between protein side chains and the MCM surface increase the conformational rigidity of protein, and immobilization of protein led to less protein aggregates.

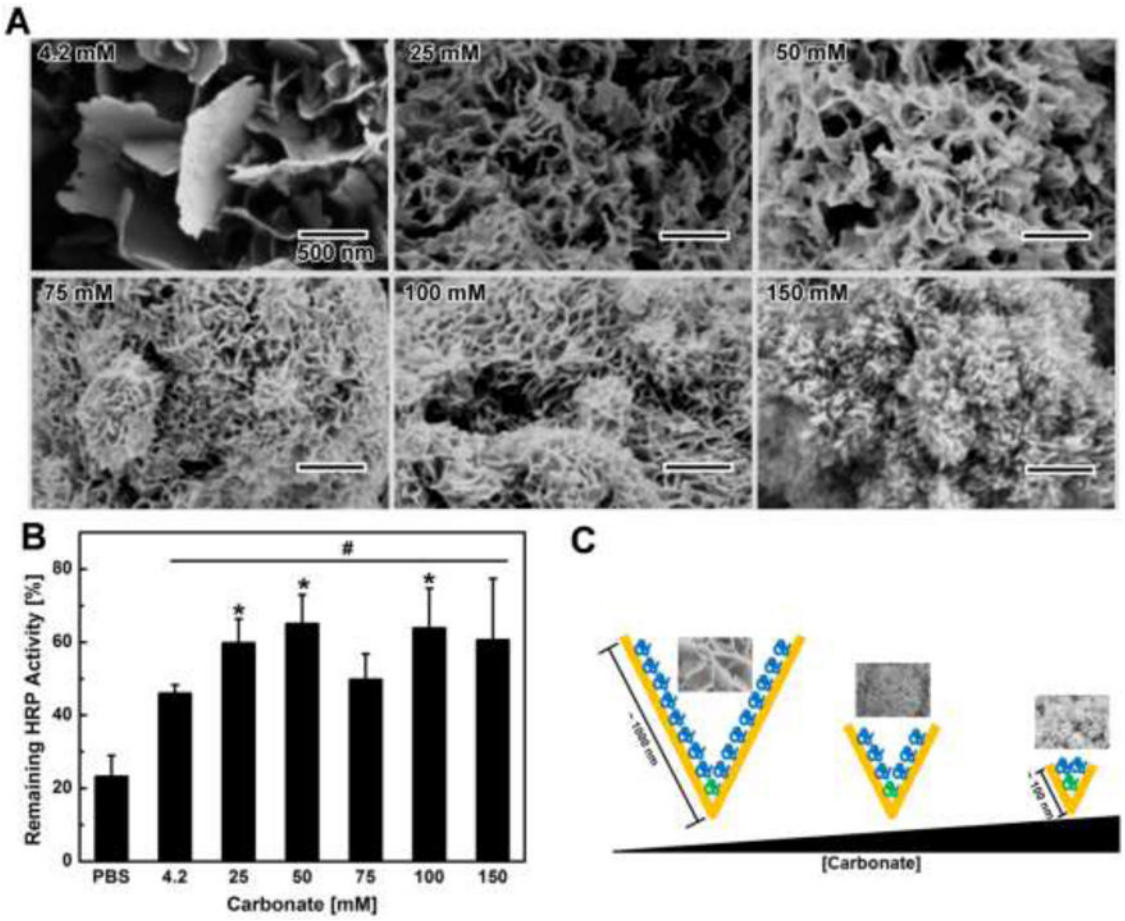

Figure 3. Impact of mineral coating nanostructure on protein stabilization

A) SEM images of MCM fabricated in mSBF with varying carbonate concentration: the size of the plate-like structure gradually decreased as the carbonate concentration increased. B) Impact of mineral coating nanostructure on HRP activity preservation: the nanoscale morphology of MCM was controlled by changing the carbonate concentration in solution during coating formation. C) Proposed mechanism of nanostructure affecting protein stabilization: plate-like structures with feature sizes closer to protein dimensions may physically trap more protein and confine protein structure within plate-like structures.

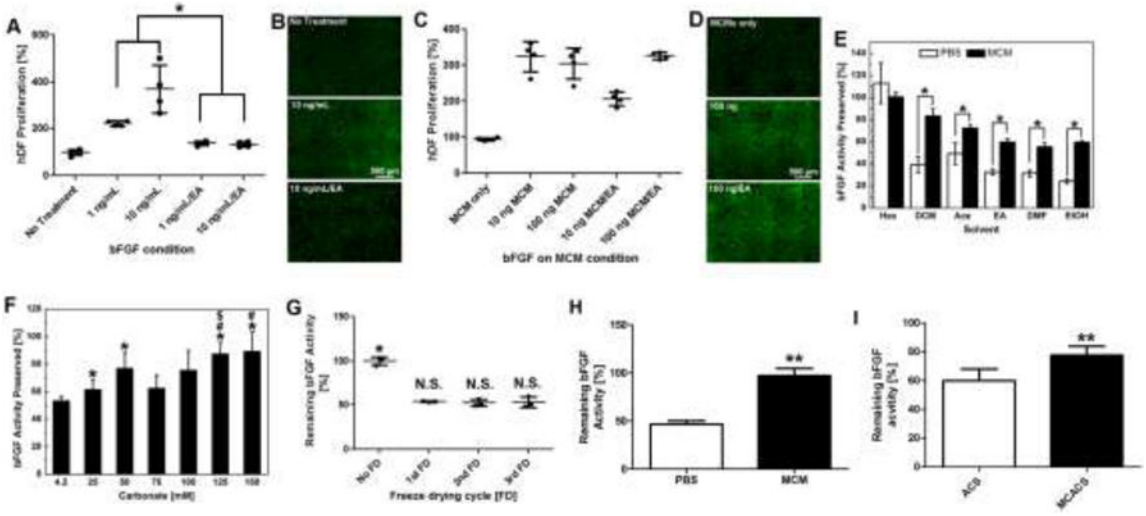

Figure 4. bFGF stabilization against organic solvents via MCM

A) bFGF activity in PBS before and after 1 h EA treatment: activity was characterized by an hDF proliferation assay. Loss of bFGF after EA treatment was shown by decreased hDF proliferation. B) Live/dead staining of hDFs treated with bFGF in PBS after 72 h. C) bFGF activity on MCMs before and after 1 h EA treatment: bFGF on MCMs could still stimulate hDF proliferation after EA treatment. D) Live/dead staining of hDF treated with different bFGFs on MCMs after 72 h. E) bFGF remaining activity after various organic solvent treatments for 4 h. F) Impact of mineral coating nanostructure on bFGF activity preservation: bFGF released from all screened MCMs showed higher activity compared to PBS. The remaining activity of bFGF was dependent on the nanostructure of MCMs. G) Remaining bFGF activity after multiple freeze drying (FD) cycles. (H) bFGF activity remained after treated by 0.05% trypsin for 1 h: bFGF bound on MCM showed little bFGF activity loss while bFGF in PBS lost over 50% of its original activity. (I) Comparison of bFGF activity on ACS with and without mineral coating: ACS was coated with a layer of mineral; bFGF was absorbed on the surface of ACS and MCACS; then treated by ethyl acetate for 2 h. Remaining bFGF activity on MCACS was significantly higher than ACS. For A, E, H, and I, data are presented as mean ± SD (n=6) *, **$p<0.05$, analyzed by Student's t-test. For F, * ($p<0.05$) represents significant difference between 4.2 mM and other tested concentrations; # ($p<0.05$) represents significant difference between 25 mM and higher concentrations; $ ($p<0.05$) represents significant difference between 75 mM and higher concentrations;

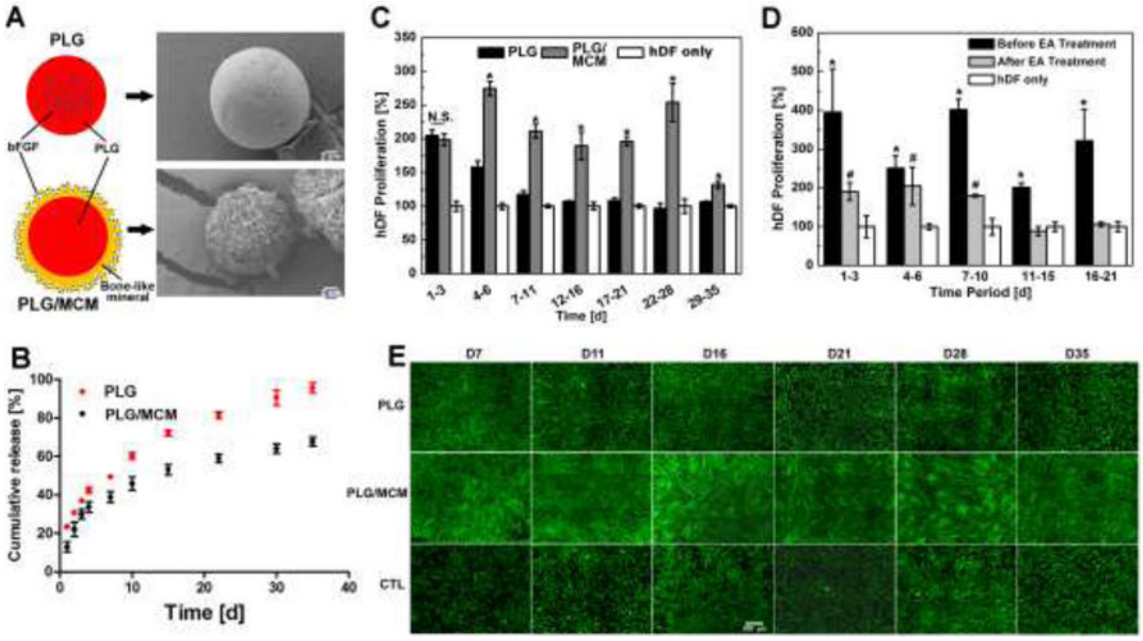

Figure 5. Comparison of bFGF released from PLG microspheres or PLG/MCM during long term delivery

A) Two bFGF delivery approaches: PLG: emulsion based encapsulation; PLG/MCM: PLG microspheres coated with mineral coating; SEM images show two types of bFGF loaded vehicles: PLG microspheres and MCMs. B) bFGF release profiles from two types of microparticles: PLG vs PLG/MCM. C) bFGF activity characterized by hDF proliferation at different stages of bFGF release: bFGF released during each time period was tested individually on hDF proliferation. Control (CTL) represents hDF receiving no treatment. D) Impact of organic solvent treatment of bFGF on long term bioactivity during delivery: bFGF bound on PLG/MCM maintained its bioactivity for only 10 days while bFGF without EA treatment kept its activity for over 21 days. For C and D, data are presented as mean ± SD (n=6) *, #, and $ $p<0.05$, analyzed by Student's t-test. E) Live/dead staining of hDF incubated with different delivery vehicles at each time point: PLG group only showed higher cell density at day 7 and 11 compared to hDF only group. In contrast, hDF cultured with PLG/MCM reached near confluence at every time point. Scale bar=500 μm

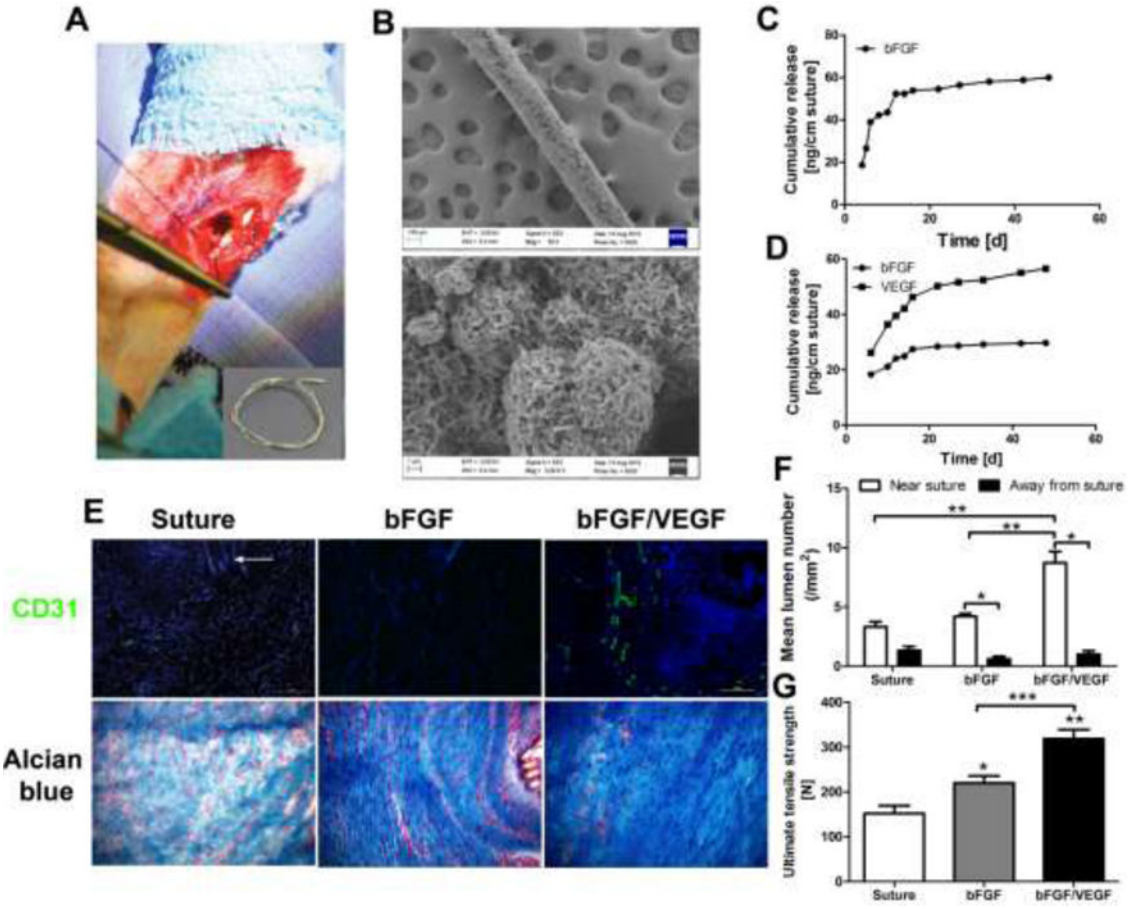

Figure 6. Growth factors stabilized and delivered via mineral-coated surgical sutures improved functional rabbit Achilles tendon healing

A) Photograph of rabbit Achilles tendon surgery: A mineral coated 4-0 USP braided nylon suture was used to create a single locking loop through the core; Inset: Gross view of a mineral coated suture. B) SEM micrographs of coated suture: High level: low magnification of suture, lower level: High magnification of mineral coating. C) bFGF release profile from mineral coated suture pulled through and knotted in tendon tissue *ex vivo*. D) bFGF/VEGF release profiles from mineral coated suture pulled through and knotted in tendon tissue *ex vivo*. E) Representative histological analysis of tendon healing after 4 weeks: improved collagen organization was observed in both growth factor treated groups while bFGF/VEGF treated group also showed more vascularization. CD31 was used as an endothelial cell marker to show vascularization at the defect sites; Alcian blue staining was used as a general histological staining to exhibit the tendon healing process with a focus on collagen fiber organization. White arrow: remaining suture at the tendon defect sites; F) Quantification of vascularization in the tendon healing area: majority of lumens appeared in the area near suture; plus, release of VEGF substantially increased the vascular in the tendon healing area. G) Ultimate tensile strength (UTS) of treated tendon after 4 weeks: UTS of both growth factor treated groups demonstrated significant mechanical property improvement compared to control group. In particular, the group treated with bFGF/VEGF incorporated suture

showed an almost two-fold increase in UTS. Six New Zealand while rabbits were used in each test group. *, **, and *** $p<0.05$, analyzed by Student's t-test.